DOI: 10.15825/1995-1191-2025-4-125-132

SILK-BASED SCAFFOLDS FOR TISSUE ENGINEERING AND RECONSTRUCTIVE SURGERY: MECHANICAL AND STRUCTURAL PROPERTIES

E.I. Podbolotova[1, 2], A.R. Pashutin[1, 2], N.V. Grudinin[1], E.A. Volkova[1], O.I. Agapova[1], A.E. Efimov[1], I.I. Agapov[1]

[1] Shumakov National Medical Research Center of Transplantology and Artificial Organs, Moscow, Russian Federation

[2] Moscow Institute of Physics and Technology, Dolgoprudny, Russian Federation

Silk is a promising natural biomaterial that combines mechanical strength, biocompatibility, and controlled biodegradation, making it highly suitable for scaffold creation for clinical practice. This study investigates how different processing methods influence the morphological and mechanical characteristics of silk-based scaffolds. The findings showed that varying the processing conditions facilitates the production of materials with tailored properties, ranging from dense, mechanically robust structures to porous, rapidly degradable scaffolds. High-density samples (Fibroplen-Atlas) exhibited substantial mechanical stability, making them promising candidates for surgical applications in mechanically demanding areas such as ligaments, fascia, and tendons. In contrast, more porous scaffolds (Fibroplen-Gas) demonstrated accelerated biodegradation, which is advantageous for soft tissue regeneration. These results highlight the potential of silk scaffolds for personalized applications, where the balance between mechanical stability and biodegradation rate can be adjusted according to specific clinical needs.

Keywords: silk fibroin, mechanical properties, tissue engineering, biomaterials.

INTRODUCTION

In recent decades, biomedical technologies aimed at restoring and replacing damaged tissues and organs have developed rapidly. A key component of these technologies is biomaterials, which form the foundation for creating implants, scaffolds, and various medical devices. The performance of these materials is determined by their biocompatibility, biodegradability, and, critically, their mechanical properties, such as strength, elasticity, and resistance to physiological stresses, which must be optimized for specific clinical applications [1, 2]. These properties directly influence the integration of the implant within the tissue environment, its functional durability, and the overall effectiveness of regeneration [3, 4].

In regenerative medicine and tissue engineering, for instance, scaffolds must possess sufficient mechanical stability to preserve the architecture of the defect and provide structural support for cell attachment and proliferation until regeneration is complete. However, the required level of mechanical strength varies considerably with the anatomical site: dense, durable materials with prolonged resorption times are necessary for the replacement of tendons, ligaments, and fascial structures, whereas more elastic, rapidly degradable matrices are preferred for soft tissue engineering applications [5, 6].

Silk fibroin, derived from the cocoons of the silkworm *Bombyx mori*, is a promising natural polymer that has been extensively studied in recent years as a foundation for developing biocompatible and biodegradable matrices in regenerative medicine and tissue engineering [7–10]. Its high mechanical strength, chemical modifiability, and low immunogenicity make silk a versatile material suitable for a broad range of medical applications – from permanent tissue replacements to temporary scaffolds that promote the restoration of native biological structures [11].

Silk fibroin is a macromolecule with an ordered architecture in which highly crystalline regions (predominantly β-sheet structures) alternate with amorphous domains. The crystalline regions form a rigid framework that imparts high mechanical strength and resistance to enzymatic degradation, whereas the amorphous regions provide flexibility and elasticity [12]. The balance between these two domains determines the overall physical and mechanical properties of fibroin, which can be precisely tuned by modifying processing conditions.

Fibroin elicits minimal inflammatory response *in vivo* and supports cell adhesion, proliferation, and differentiation, especially with additional surface modification or when supplemented with bioactive molecules [13–17].

One of the key advantages of silk fibroin lies in its versatility and technological flexibility. By varying pro-

Corresponding author: Igor Agapov. Address: 1, Shchukinskaya str., Moscow, 123182, Russian Federation. Phone: (495) 231-60-42. E-mail: igor_agapov@mail.ru

cessing conditions, such as solvent composition, extraction time, and thermal or mechanical treatment, it is possible to deliberately tailor the morphology, degree of crystallinity, porosity, biodegradation rate, and mechanical performance of the material [18, 19]. This tunability enables the adaptation of silk-based scaffolds to a wide range of clinical applications.

The present study aims to elucidate the relationship between the extent of silk processing and the resulting changes in the mechanical and morphological characteristics of fibroin-based scaffolds. The primary objective is to determine how different fabrication approaches influence scaffold properties, thereby providing a rationale for selecting optimal processing parameters to create biomaterials that meet specific clinical requirements. This will allow for targeted design of scaffold types – ranging from dense, slowly resorbable structures to porous, rapidly degradable matrices – depending on the intended surgical application.

MATERIALS AND METHODS

Obtaining samples

Natural silk fabrics (EAC Declaration of Conformity, N RU D-CN.PA09.B.91575/23, Tianjin Textile Industrial Supply and Sale Co., Ltd., China) were used for the preparation of biodegradable scaffolds. Two types of silk fabrics differing in surface density – 15 g/m^2 and 155 g/m^2 – were employed in this study. Sample preparation was carried out according to previously described protocols [20–22].

The processing procedure included several sequential stages. Initially, the silk fabric was boiled in a 0.25% aqueous sodium bicarbonate ($NaHCO_3$) solution for 40 minutes in a water bath to remove sericin, followed by thorough rinsing in distilled water. The fabric was then reboiled in a fresh $NaHCO_3$ solution for 30 minutes, and this process was repeated three times to ensure complete sericin removal. After treatment, the samples were air-dried at room temperature until a constant weight was achieved.

The resulting materials were designated as “Fibroplen-Gas” (15 g/m^2) and “Fibroplen-Atlas” (155 g/m^2). These samples were used as model scaffolds for subsequent analyses.

Obtaining the solution

The purified silk fabrics were dissolved in a mixture of distilled water, 95% ethanol, and calcium chloride (Sharlab S.L., Spain) in a molar ratio of 8 : 2 : 1, respectively. The volume of the mixture was calculated at 1 mL of solution per 200 mg of fibroin. Dissolution was carried out in sealed test tubes at 90 °C for 40 minutes with constant stirring until a homogeneous solution was obtained.

The resulting solution was purified from calcium chloride and ethanol by dialysis against distilled water at 20 °C, with ten water changes performed at 30-minute intervals. Upon completion of dialysis, the solution was further purified by centrifugation at 3000 rpm for 15 minutes using a SIGMA 6K10 2000 W centrifuge (Sigma, Germany) to remove insoluble particles. The resulting solution was subsequently subjected to mass spectrometric analysis to verify its protein composition, assess its purity, and confirm its suitability for further use.

Mass spectrometry

An aliquot of the solution containing 20 μg of total protein was dried in a SpeedVac centrifugal vacuum concentrator (Savant, France) and resuspended in 20 μL of buffer containing 100 mM Tris-HCl (pH 8.5), 1% sodium deoxycholate, 10 mM TCEP, and 20 mM 2-chloroacetamide. The mixture was incubated at 85 °C for 10 minutes and subsequently cooled to room temperature. 0.4 μg of trypsin in 10 μl of 100 mM Tris-HCl (pH 8.5) was added to the solution, and the reaction mixture was incubated at 37 °C overnight. The reaction was terminated by adding an equal volume of 2% trifluoroacetic acid (TFA), after which the peptides were purified by solid-phase extraction on an SDB-RPS StageTip microcolumn made from an automatic pipette tip packed with SDB-RPS membrane (3M, USA). The column was sequentially washed with 1% TFA in ethyl acetate and 0.2% TFA in water, and peptides were eluted using 5% ammonium hydroxide in 60% acetonitrile. The eluate was dried completely and stored at –80 °C. Prior to analysis, peptides were reconstituted in 0.1% TFA and 2% acetonitrile in water.

Chromatographic–mass spectrometric analysis was performed on an Ultimate 3000 Nano LC system (Thermo Fisher Scientific) coupled to an Orbitrap Lumos Tribrid mass spectrometer (Thermo Fisher Scientific) via a nanoelectrospray ionization source. Peptides were first loaded onto a precolumn packed with Reprosil-Pur C18-AQ 5 μm sorbent and subsequently separated on a fused silica analytical column packed with Reprosil-Pur C18-AQ 1.9 μm sorbent. Chromatographic separation was carried out at room temperature using a binary solvent system: eluent A – 0.1% formic acid in water, and eluent B – 80% acetonitrile with 0.1% formic acid. Peptides were eluted with a linear gradient from 3% to 99% eluent B over 37 minutes at a flow rate of 500 nL/min.

The mass spectrometer operated in data-dependent acquisition (DDA) mode with the following parameters: MS1 resolution 60,000, mass range 350–1600 m/z, HCD fragmentation energy 30%, and MS2 resolution 15,000.

Data processing was performed using MaxQuant (v.2.4.2.0) and Perseus (v.2.0.10.0) software packages. Database searching was carried out against the *Bombyx mori* protein sequence database (UniProt, version 04.2025) using standard MaxQuant settings: trypsin

specificity, up to two missed cleavages, variable modifications (methionine oxidation, N-terminal acetylation), fixed modification (cysteine carbamidomethylation), and a false discovery rate (FDR) threshold of 1% at both peptide and protein levels.

Subsequent data analysis in Perseus included the exclusion of contaminants, reverse sequences, and proteins identified only by site. Relative protein quantification was performed using the relative intensity-based absolute quantification (iBAQ) algorithm.

Obtaining modified samples

Fibroplen-Gas and Fibroplen-Atlas samples were incubated in an aqueous–alcoholic solution of calcium chloride ($CaCl_2$) with a molar ratio of $CaCl_2$: ethanol : water = 1 : 2 : 8 at 46 °C. The treatment was continued until the complete loss of fabric integrity. The time required for full structural disintegration was 7 hours for Fibroplen-Gas and 4.5 hours for Fibroplen-Atlas samples; these durations were defined as representing 100% destruction.

Based on these reference points, incubation times corresponding to 20%, 40%, 60%, and 80% degrees of destruction were calculated proportionally. Upon completion of each treatment, the samples were thoroughly rinsed with distilled water to remove residual reagents and subsequently air-dried at room temperature until a constant weight was achieved.

The resulting scaffolds were sterilized in a Sanyo MLS-3020U autoclave (Sanyo, Japan) at 126 °C for 30 minutes. The modified scaffolds were designated with numerical indices reflecting the percentage of structural destruction.

Scanning electron microscopy

To compare the structural features of samples with different degrees of processing and to identify changes in surface morphology and microstructure resulting from tissue modification, the samples were examined using scanning electron microscopy (SEM). The samples were dehydrated by sequential immersion in ethanol solutions of increasing concentration (10%, 20%, 50%, 70%, and 95%), with each step lasting 30 minutes. After dehydration, the samples were mounted on glass slides and vacuum-dried for 1 hour using a Q150R ES rotary pump sputtering system (Quorum Technologies, UK). The dried samples were then coated with a 5 nm layer of gold under an argon atmosphere at an ion current of 20 mA and a pressure of 1 mbar, using the same Q150R ES system (Quorum Technologies, UK). Microscopic examination was carried out with a Tescan Vega3 SBU scanning electron microscope (Tescan, Czech Republic) operated at a voltage of 30 kV. The images were captured using VegaTC software (Tescan, Czech Republic).

Mechanical properties of samples

To assess the strength characteristics of the silk scaffolds, tensile tests were conducted using a universal tensile testing machine I1158M-2 (Tochpribor, Russia). Five rectangular specimens, each measuring 8 cm × 2.5 cm, were prepared from each type of fabric. The samples were fixed in the machine's clamps and subjected to uniaxial tensile loading at a crosshead speed of 50 mm/min until they broke. During the test, the relationship between the applied load and elongation was continuously measured. The tensile strength of each sample was calculated based on the maximum load at break and the corresponding strain.

Data processing

All quantitative data are presented as mean ± standard deviation (M ± SD). The Mann–Whitney U test was applied to evaluate statistical differences between groups. Differences were considered statistically significant at $p < 0.05$. Data analysis and graphical visualization were performed using OriginPro software (OriginLab Corporation, USA).

RESULTS AND DISCUSSION

Mass spectrometry analysis

Mass spectrometric analysis of the fibroin solution obtained from sericin-free satin silk tissue identified 50 protein sequence groups corresponding to *Bombyx mori* silk proteins (according to the UniProt database, version 04.2025). Protein identification and quantification performed using MaxQuant revealed that more than 97% of the total molar protein content was represented by fibroin light chains (42.3%), fibroin heavy chains (48.8%), and fibrohexamerin (P25) (6.1%). This composition corresponds closely to the native protein profile of fibroin extracted from *Bombyx mori* cocoons, confirming the high preservation of the native structure of silk after processing and confirms that the solution contains predominantly pure fibroin. Thus, it can be concluded that the pretreated silk tissue matrices retain the native biochemical composition characteristic of natural fibroin and can be used as a basis for creating biocompatible scaffolds.

Tissue morphology

SEM analysis of the samples revealed a clear relationship between the microstructural characteristics of the samples and the degree of modification. In the untreated samples, the fibers exhibited a dense and orderly arrangement with a smooth surface, retaining both their structural integrity and spatial organization. This was particularly evident in the samples with a denser weave (Fibroplen-Atlas). As the degree of processing increased (from 20% to 80%), progressive structural alterations were observed. The fiber surfaces became roughened,

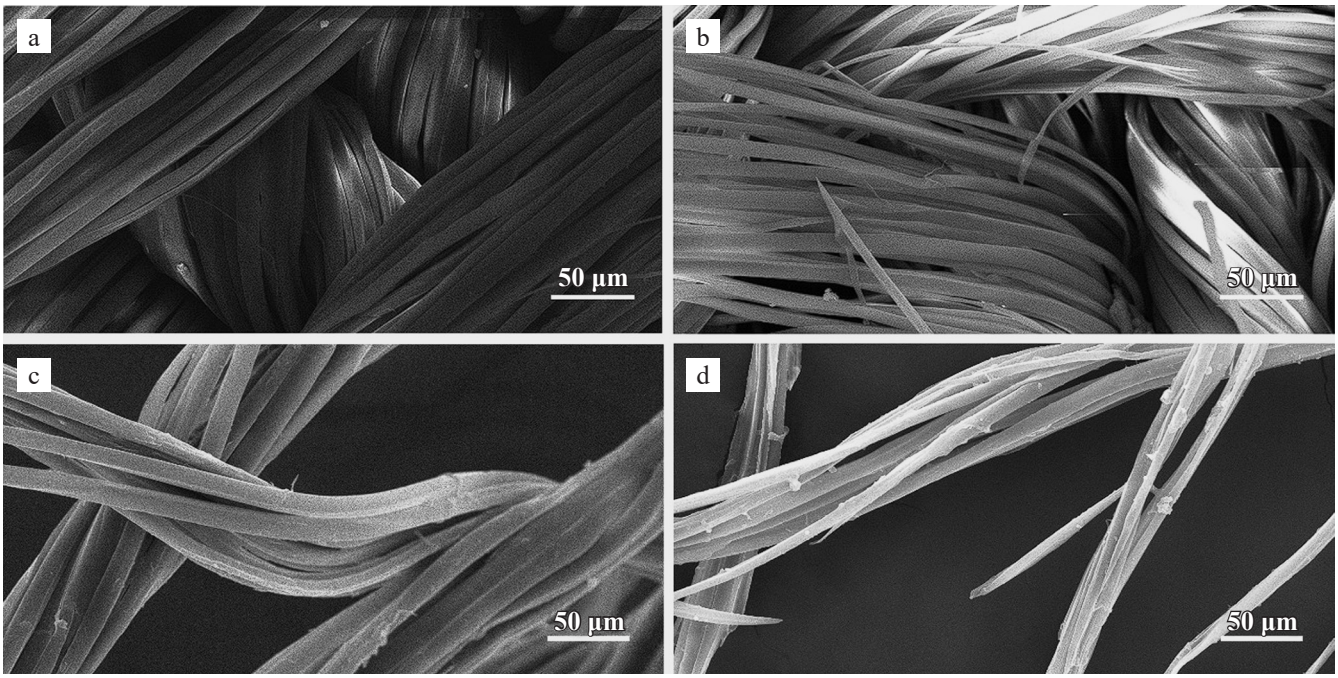

Fig. 1. Surface morphology of silk fabrics at different processing levels, according to scanning electron microscopy (SEM). a, Fibroplen-Atlas; b, Fibroplen-Atlas 80; c, Fibroplen-Gas; d, Fibroplen-Gas 80

Table

Tensile strength of silk scaffolds at different degrees of modification

Sample	Tensile strength (MPa)
A0	34.67 ± 2.80
A20	28.11 ± 2.30
A40	21.30 ± 1.90
A60	17.68 ± 1.50
A80	15.04 ± 1.30

Sample	Tensile strength (MPa)
G0	9.01 ± 0.80
G20	8.97 ± 0.80
G40	8.12 ± 0.70
G60	7.32 ± 0.65
G80	7.86 ± 0.70

with evident localized degradation, loosening of the network, and regions of thinning. Breaks formed in the fibrous network. At higher modification levels, the structure became less ordered, and the fabric became more porous and fragile (Fig. 1).

Mechanical properties

Mechanical testing of the silk scaffolds revealed pronounced differences in tensile strength, reflecting the influence of fabric density and structural organization on the mechanical behavior of the materials. The untreated Fibroplen-Atlas (A0) samples showed a maximum tensile strength of 34.67 ± 2.80 MPa (Fig. 2), which was significantly higher than that of the modified samples (A20–A80), where tensile strength varied from 28.11 ± 2.30 MPa to 15.04 ± 1.30 MPa. The Fibroplen-Gas samples, with lower fabric density, showed considerably reduced strength. The untreated G0 samples had a maximum tensile strength of 9.01 ± 0.80 MPa, which decreased to 7.86 ± 0.70 MPa following maximal modification (G80) (Table).

For Fibroplen-Atlas samples, a clear and statistically significant ($p < 0.05$) inverse relationship was observed between tensile strength and degree of processing. Increasing the incubation time in the calcium chloride–ethanol solution led to a gradual decline in mechanical strength, indicating progressive structural degradation of the fibroin matrix. A similar trend was noted for the Fibroplen-Gas samples, although with greater data variability.

DISCUSSION

The observed decrease in tensile strength with increasing degrees of modification is attributed to the partial disruption of the fibroin protein matrix, resulting in reduced structural integrity and mechanical stability of the scaffolds. This finding is consistent with previous studies [20, 22], which have shown that chemical processing of silk fibroin leads to a loss of crystallinity and partial unfolding of β-structures, thereby diminishing the strength of the material while accelerating its biodegradation.

The high-density Fibroplen-Atlas samples demonstrated superior mechanical performance, making them suitable for use in surgical applications that require long-

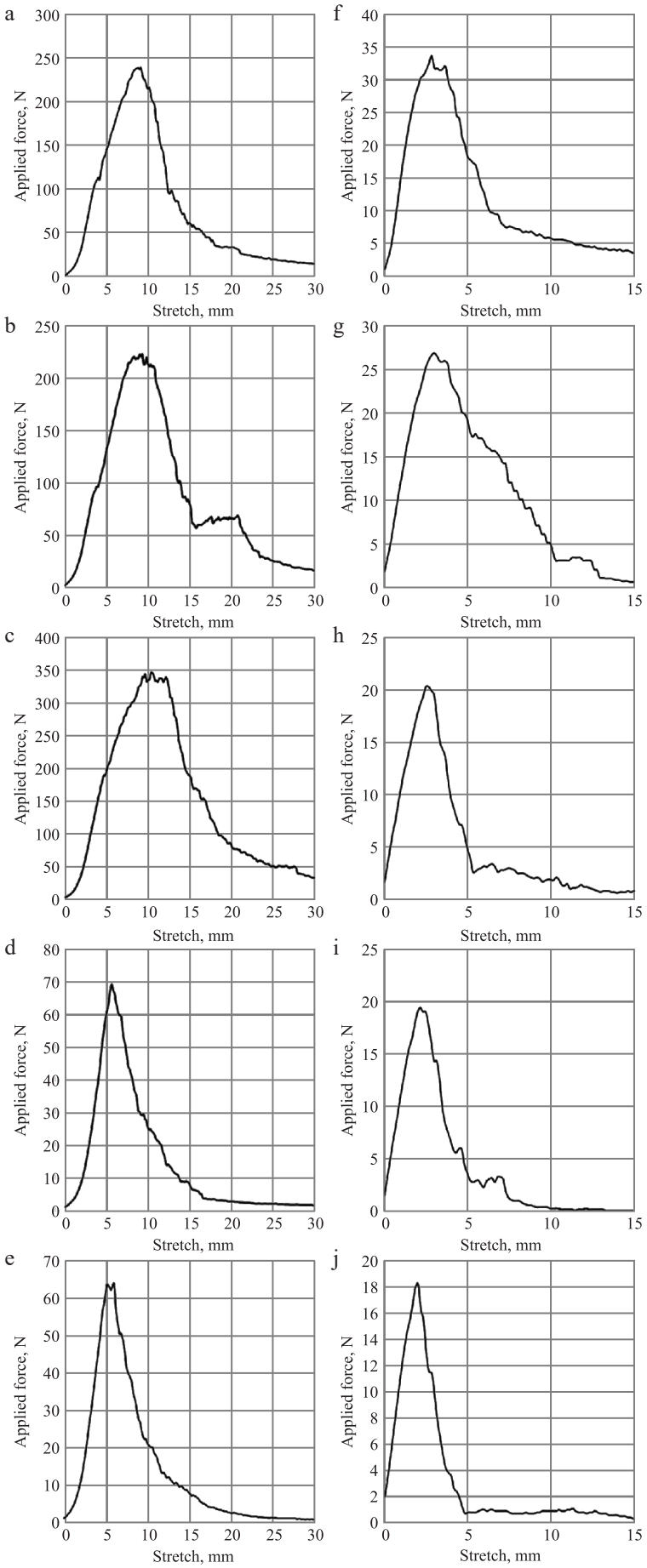

Fig. 2. Dependence of breaking force on time from the start of testing for silk scaffold samples A0–A80 (a–e) and G0–G80 (f–j). The maximum recorded value is taken as the breaking force of the scaffold

term mechanical reinforcement, such as tendon, fascia, and other structures subjected to significant stress, where it is necessary to maintain the stability of the framework for a long time after surgery, for example, in orthopedics and reconstructive surgery.

Indeed, high-strength silk matrices are already employed clinically in procedures such as rotator cuff reconstruction and knee ligament repair, where prolonged stability and resistance to stress are critical to successful postoperative outcomes [23–26].

At the same time, Fibroplen-Gas samples, characterized by a looser and more porous architecture, exhibited lower mechanical strength but a faster biodegradation rate, making them ideal for soft tissue surgery. Such materials hold promise for use in regenerative medicine, particularly for wound coverage, burn treatment, and plastic surgery, where temporary biodegradable matrices are required for accelerated epithelial and vascular growth.

CONCLUSION

This study demonstrated that physicochemical treatment of silk tissues exerts a pronounced influence on their morphological and mechanical properties, enabling the formation of scaffolds with distinct architectural characteristics. By varying treatment parameters, it was possible to obtain biomaterials with a controlled degree of protein matrix degradation, which in turn determined their mechanical strength and expected biodegradation kinetics.

High-density scaffolds fabricated from materials such as Fibroplen-Atlas exhibit pronounced mechanical strength and structural stability, making them highly promising for clinical applications that require long-term tissue support. In contrast, scaffolds with a less dense architecture (such as Fibroplen-Gas) display lower tensile strength but increased biodegradation rates, rendering them more suitable for use in tissue engineering and regenerative surgery, including the treatment of chronic wounds, burns, and creation of matrices.

Thus, the developed silk-based scaffolds demonstrate significant potential for adaptive use in clinical practice, where selection of material can be guided by the biomechanical demands of the target tissue and the desired rate of regeneration. The results confirm the feasibility of targeted modulation of the properties of silk biomaterials to meet specific therapeutic objectives.

ACKNOWLEDGEMENTS

The authors would like to thank Rustam H. Ziganshin for his assistance in performing the mass spectrometry analyses.

The authors declare no conflict of interest.

REFERENCES

1. *Wang L, Wang C, Wu S, Fan Y, Li X*. Influence of mechanical properties of biomaterials on degradability, cell behaviors and signaling pathways: current progress and challenges. *Biomater Sci*. 2020 May 21; 8 (10): 2714–2733. doi: 10.1039/d0bm00269k.
2. *Binyamin G, Shafi BM, Mery CM*. Biomaterials: A primer for surgeons. *Semin Pediatr Surg*. 2006 Nov; 15 (4): 276–283. doi: 10.1053/j.sempedsurg.2006.07.007.
3. O'Brien FJ. Biomaterials & scaffolds for tissue engineering. Materials Today. 2011; 14 (3): 88–95. doi: 10.1016/S1369-7021(11)70058-X.
4. *Efimov AE, Agapova OI, Safonova LA, Bobrova MM, Parfenov VA, Koudan EV et al.* 3D scanning probe nanotomography of tissue spheroid fibroblasts interacting with electrospun polyurethane scaffold. *Express Polymer Letters*. 2019; 13 (7): 632–641. doi: 10.3144/expresspolymlett.2019.53.
5. *Chan BP, Leong KW*. Scaffolding in tissue engineering: general approaches and tissue-specific considerations. *Eur Spine J*. 2008 Dec; 17 (Suppl 4): 467–479. doi: 10.1007/s00586-008-0745-3.
6. *Suamte L, Tirkey A, Barman J, Jayasekhar Babu P.* Various manufacturing methods and ideal properties of scaffolds for tissue engineering applications. *Smart Materials in Manufacturing*. 2023; 1: 100011. doi: 10.1016/j.smmf.2022.100011.
7. *Podbolotova EI, Agapova OI*. Biodegradable silk-based products for regenerative medicine. *Russian Journal of Transplantology and Artificial Organs*. 2024; 26 (4): 157–165. [In Russ, English abstract]. doi: 10.15825/1995-1191-2024-4-157-165.
8. *Prokudina ES, Senokosova EA, Antonova LV, Krivkina EO, Velikanova EA, Akentieva TN et al.* New Tissue-Engineered Vascular Matrix Based on Regenerated Silk Fibroin: *in vitro* Study. *Sovrem Tekhnologii Med*. 2023; 15 (4): 41–48. doi: 10.17691/stm2023.15.4.04. PMID: 38434192.
9. *Mantry S, Silakabattini K, Das PK, Sankaraiah J, Barik CS, Panda S et al*. Silk fibroin: An innovative protein macromolecule-based hydrogel/ scaffold revolutionizing breast cancer treatment and diagnosis – Mechanisms, advancements, and targeting capabilities. *Int J Biol Macromol*. 2025 Apr 5; 309 (Pt 2): 142870. doi: 10.1016/j.ijbiomac.2025.142870. PMID: 40194579.
10. *Sun W, Gregory DA, Tomeh MA, Zhao X*. Silk Fibroin as a Functional Biomaterial for Tissue Engineering. *Int J Mol Sci*. 2021 Feb 2; 22 (3): 1499. doi: 10.3390/ijms22031499. PMID: 33540895.
11. *De Giorgio G, Matera B, Vurro D, Manfredi E, Galstyan V, Tarabella G et al.* Silk Fibroin Materials: Biomedical Applications and Perspectives. *Bioengineering (Basel)*. 2024 Feb 9; 11 (2): 167. doi: 10.3390/bioengineering11020167. PMID: 38391652.
12. *Qi Y, Wang H, Wei K, Yang Y, Zheng RY, Kim IS, Zhang KQ*. A Review of Structure Construction of Silk Fibroin Biomaterials from Single Structures to Multi-Level Structures. *Int J Mol Sci*. 2017 Mar 3; 18 (3): 237. doi: 10.3390/ijms18030237. PMID: 28273799.

13. *Tian Z, Chen H, Zhao P*. Compliant immune response of silk-based biomaterials broadens application in wound treatment. *Front Pharmacol*. 2025 Feb 12; 16: 1548837. doi: 10.3389/fphar.2025.1548837.
14. *Jacobsen MM, Li D, Rim NG, Backman D, Smith ML, Wong JY*. Silk-fibronectin protein alloy fibres support cell adhesion and viability as a high strength, matrix fibre analogue. *Sci Rep*. 2017 Apr 5; 7: 45653. doi: 10.1038/srep45653.
15. *Safonova L, Bobrova M, Efimov A, Lyundup A, Agapova O, Agapov I.* A Comparative Analysis of the Structure and Biological Properties of Films and Microfibrous Scaffolds Based on Silk Fibroin. *Pharmaceutics*. 2021 Sep 26; 13 (10): 1561. https://doi.org/10.3390/pharmaceutics13101561.
16. *Safonova L, Bobrova M, Efimov A, Davydova L, Tenchurin T, Bogush V et al.* Silk Fibroin/Spidroin Electrospun Scaffolds for Full-Thickness Skin Wound Healing in Rats. *Pharmaceutics*. 2021 Oct 15; 13 (10): 1704. doi: 10.3390/pharmaceutics13101704.
17. *Gavrilova NA, Borzenok SA, Revishchin AV, Tishchenko OE, Ostrovkiy DS, Bobrova MM et al.* The effect of biodegradable silk fibroin-based scaffolds containing glial cell line-derived neurotrophic factor (GDNF) on the corneal regeneration process. *Int J Biol Macromol*. 2021 Aug 31; 185: 264–276. doi: 10.1016/j.ijbiomac.2021.06.040.
18. *Cao Y, Wang B*. Biodegradation of Silk Biomaterials. *Int J Mol Sci*. 2009 Mar 31; 10 (4): 1514–1524. doi: 10.3390/ijms10041514.
19. *Koh LD, Cheng Y, Teng CP, Khin YW, Loh XJ, Tee SY et al.* Structures, mechanical properties and applications of silk fibroin materials. *Progress in Polymer Science*. 2015 Jul; 46: 86–110. doi: 10.1016/j.progpolymsci.2015.02.001.
20. *Podbolotova EI, Pashutin AR, Efimov AE, Agapova OI, Agapov II*. *In vitro* Degradation Study of Tissue-Based Materials from Natural Silk for Regenerative Medicine. *Biomaterials*. 2024; 40 (3): 95–99. [In Russ, English abstract]. doi: 10.56304/S0234275824030104.
21. *Agapov II, Agapova OI, Efimov AE, Sokolov DYu, Bobrova MM, Safonova LA.* Sposob polucheniya biodegradiruemykh skaffoldov na osnove tkaney iz natural'nogo shelka. Patent na izobretenie RU2653428 S1, 08.05.2018.
22. *Agapov II, Podbolotova EI, Kirsanova LA, Grudinin NV, Pashutin AR, Agapova OI et al*. *In vitro* and *in vivo* Biodegradation of Silk Fabric Scaffolds. *Dokl Biol Sci*. 2025 Feb; 520 (1): 34–37. doi: 10.1134/S0012496624600519.
23. *Zheng Z, Ran J, Chen W, Hu Y, Zhu T, Chen X et al.* Alignment of collagen fiber in knitted silk scaffold for functional massive rotator cuff repair. *Acta Biomater*. 2017 Mar 15; 51: 317–329. doi: 10.1016/j.actbio.2017.01.041. PMID: 28093363.
24. *Chen X, Qi YY, Wang LL, Yin Z, Yin GL, Zou XH, Ouyang HW.* Ligament regeneration using a knitted silk scaffold combined with collagen matrix. *Biomaterials*. 2008 Sep; 29 (27): 3683–3692. doi: 10.1016/j.biomaterials.2008.05.017.
25. *Shang P, Xiang Y, Xing C, Chen S, Yuan F*. Procyanidin-crosslinked gradient silk fibroin composite nanofiber scaffold with sandwich structure for rotator cuff repair. *Biomater Adv*. 2025 Apr; 169: 214183. doi: 10.1016/j.bioadv.2025.214183.
26. *Fan H, Liu H, Wang Y, Toh SL, Goh JC*. Development of a silk cable-reinforced gelatin/silk fibroin hybrid scaffold for ligament tissue engineering. *Cell Transplant*. 2008; 17 (12): 1389–1401. doi: 10.3727/096368908787648047.

The article was submitted to the journal on 10.06.2025